CASE STUDY

Experimental Optimization of Computer Models of Manufacturing Processes

Bruce Ankenman, Søren Bisgaard, and Tim A. Osswald
Center for Quality and Productivity Improvement, Department of Industrial Engineering and Department of Mechanical Engineering, University of Wisconsin-Madison, Madison, WI 53705

COMPUTER MODELS OF A PRODUCT OR PROCESS THAT IS BEING DEVELOPED CAN FACILITATE EFFORTS TO REDUCE DEVELOPMENT TIME AND COST. HOWEVER, THE USE OF COMPUTER SIMULATION MODELS IS OFTEN LIMITED TO AD HOC, ONE-FACTOR-AT-A-TIME EXPLORATION RATHER THAN SYSTEMATIC OPTIMIZATION. IN THIS ARTICLE, THE AUTHORS USE A COMPRESSION MOLDING PROCESS MODEL TO DEMONSTRATE A SEQUENTIAL STRATEGY BASED ON RESPONSE SURFACE METHODOLOGY THAT CAN BE USED FOR OPTIMIZING COMPLEX COMPUTER MODELS.

During the past decade, spectacular improvement in computer technology has fundamentally changed the way engineers work. Today, computer simulation of physical processes has become a standard tool of many design and manufacturing engineers. Powerful computer-aided design (CAD) tools, finite element analysis (FEA) programs, spreadsheets, and high-level deterministic and stochastic simulation packages make possible computations and detailed analyses of engineering problems not dreamed of just a few years ago. The earlier these tools are put to use in the product development cycle, the more impact they will have. Ideally, they will be used during the initial product and process design.

In the design phase, it is important to be able to compute or simulate the consequences of a given set of engineering specifications. However, once it is possible to evaluate the consequences of the specifications, the next question is, "What happens if we change the specifications?" In other words, how sensitive (or rugged or robust) is the design to changes in the specifications and, taking this one step further, what is the predicted optimum design? It is this

second stage of sensitivity analysis and optimization of complex computer models, often called computer experimentation, that we discuss in this article.

Most engineers conduct computer experiments using a "one-factor-at-a-time" approach, changing each factor in turn while leaving all others constant. This approach is highly inefficient, not very systematic, and may not lead to an optimum design solution. As an alternative, it has been suggested that an approximate prediction function be developed for a complex computer model. This simpler function can then be used to find the best design [1]. However, for optimization it is not necessary to find a prediction function for the entire range of the computer model. Instead, if the response is reasonably well behaved, we only need to determine the local gradient and then iteratively pursue the direction of maximum benefit.

In this article, we demonstrate an iterative optimization approach, based on the philosophy and related statistical techniques of response surface methodology (RSM) [2, 3], a "hill-climbing" optimization technique developed and used extensively in physical experimentation [4]. In RSM, the response surface is defined as the set of all possible response values. RSM typically starts with the experimenter's best guess for factor settings and then uses designed experiments to "climb" the response surface until a local optimum is reached. There is no guarantee that this is a global optimum, and some other starting point may yield a different local optimum. However, in many cases the experimenter's best guess for factor conditions is the only reasonable starting point. Thus, unless one is willing to risk running extraneous experiments finding other local optima which are likely to be less desirable, the local optima is accepted as a significant quality improvement and the experiment is ended. The RSM approach, in the context of computer experiments, provides engineers with two important benefits. First, it is a systematic and efficient way to find a good starting point for prototyping. Second, RSM provides valuable information about how the design factors affect the response in the region around the computer generated optimum point.

To demonstrate our approach, we apply RSM to a finite element model of the material flow of a compression molding process. We first provide a discussion of a finite element analysis model. Then we show, step-by-step, the use of RSM for finding an optimum starting location for a prototype molding process. After the optimum conditions are reached, we provide an analysis of the geometry of the response surface near the predicted optimum. Finally, we discuss the general applicability of the sequential approach for the optimization of complex computer models. We have chosen a relatively simple example to demonstrate the concepts. However, the example illustrates the general idea of optimization of complex computer models of products and processes.

TECHNICAL BACKGROUND FOR THE EXAMPLE

The auto industry is increasingly using compression-molded, fiber-reinforced polymer components in their products. A typical example, which we will use for our demonstration, is a hood scoop. For the production of high quality parts, it is important to understand the flow pattern of the material during the molding process because undesirable flow patterns can lead to cracks and surface blemishes. The automobile hood scoop used for our example is shown in Figure 1.

Finite element modeling is a computer-intensive method of approximating a complicated system through time and space, by breaking it down into a mesh of small elements and finding approximate solutions to the governing differential equations for each element. In our case, the governing equations are the conservation of mass and momentum, and the parameters being calculated are pressure, velocity, and node filling time. For our computations, we used CADPRESS, a finite element/control volume simulation package [5].

The finite element mesh of the hood scoop used for the analysis is shown in Figure 2. Because of the symmetry of the product, it was only necessary to simulate half of the mold. The left half-mold represented in Fig. 2 was approximately 66 centimeters in length and 32 centimeters in width. The charge being used before our optimization, referred to as the original charge, is highlighted in the center of Fig. 2. Each element (triangular area in Fig. 2) of the mesh is numbered and was used for the calculation of the material pressure, velocity, and fiber orientation as the mold fills. The time from the beginning of the simulation until the flow front crosses each node (line vertex in Fig. 2) was called the *filling time* of that node, and these times were recorded by the computer during the simulation.

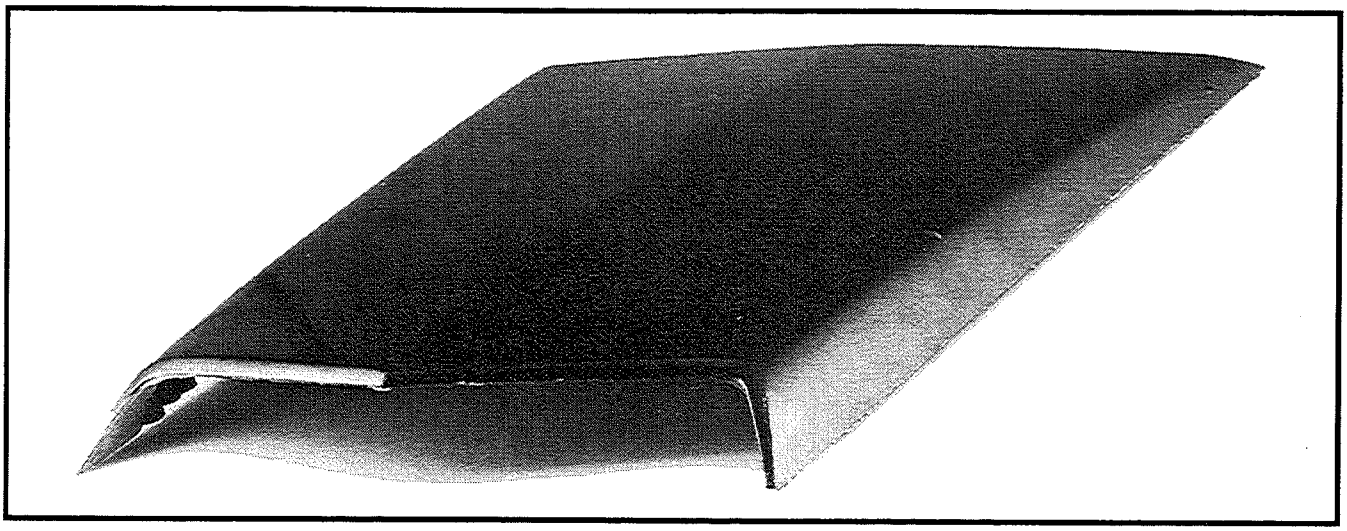

Fig. 1. The hood scoop.

Figures 3 and 4 display sample graphical output of the simulation model showing the flow pattern and fiber orientation, respectively, for the original charge. The fiber orientation of the final part, shown in Fig. 4, was represented by figure eight-shaped symbols which are polar plots of the fiber orientation distribution of each element. The length of the symbol placed in each element shows the extent of fiber orientation, and the direction of the symbol shows the main angle of orientation in that element. A short symbol indicates random orientation, and a long symbol represents highly oriented fibers in that element.

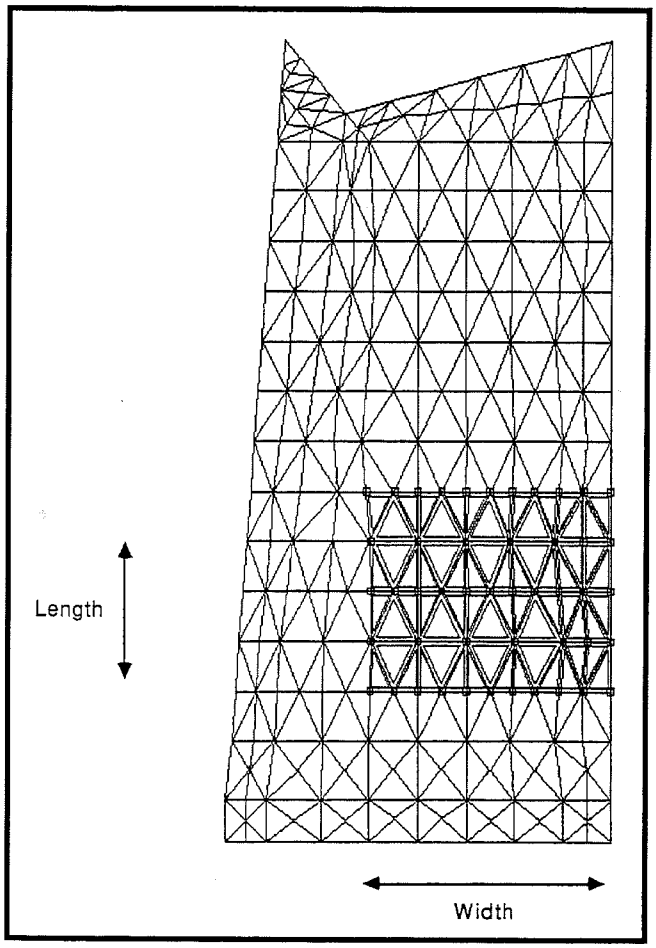

Fig. 2. The finite element mesh and the original charge.

OBJECTIVES AND RESPONSES

Experience, as well as theoretical studies, shows that random (uniform) orientation of the fibers in the polymer provides more homogeneous strength in the finished part. Important factors influencing the fiber orientation in the molded part are charge size, shape, and placement in the mold. Before the start of the compression molding, the fibers are assumed to be oriented randomly and uniformly. However, due to the material's flow and depending on the type of flow generated, the fibers have a tendency to become oriented in particular directions during compression, making the product susceptible to breakage [6].

Although completely impractical, one way to ensure random orientation in the final part is to use a charge that is identical to the final shape. This, of

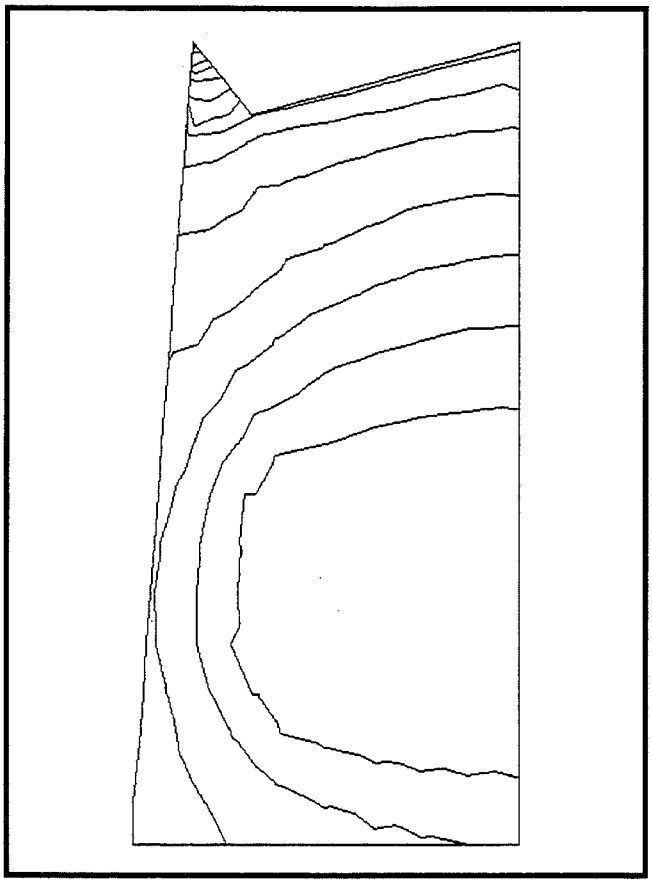

Fig. 3. Flow of the original charge.

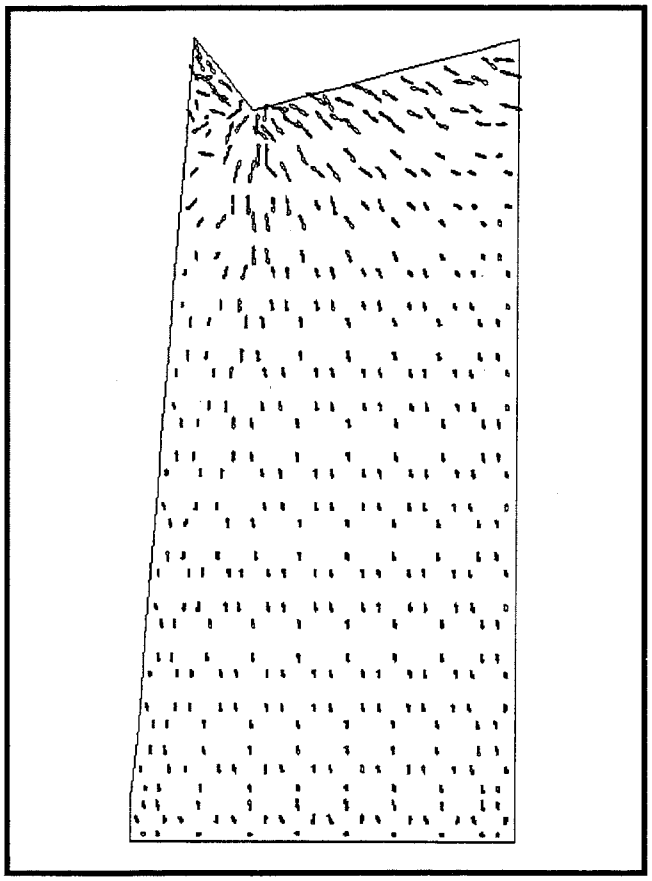

Fig. 4. Fiber orientation of the original charge.

course, is not a useful solution since material flow is required to obtain the shape of the product and to achieve smooth surface characteristics. To ensure substantial flow during molding, we imposed the constraint that the charge area should be no more that 30% of the mold area.

In addition to the pictorial responses of Figs. 3 and 4 that qualitatively show the mold filling and the fiber orientation, two numerical responses were developed to quantify these responses. The first numerical response indicates the uniformity of the mold filling. Uniform mold filling is important in order to reduce the velocity gradients which cause fiber orientation. Ideally, every point on the flow front should reach the mold wall at the same time, but in practice the mold wall filling times will vary. To control filling uniformity, we therefore developed a numerical response, called *fill time tolerance*, which is proportional to the standard deviation of the filling times of all of the mold wall nodes. To increase uniformity in mold filling and thus more random fiber orientation, the fill time tolerance should be minimized. For the original charge, the model predicted a fill time tolerance of 1.129 seconds.

A second response was the *average fiber orientation*. This response was computed by first finding the height of the peak in the distribution of fiber directions in each element. These heights indicate the extent of fiber orientation in each element and determine the length of the figure eight-shaped symbols in each element in Fig. 4. We then averaged these heights across all elements to obtain the average fiber orientation. For the original charge, the average fiber orientation had a numerical value of 0.849.

EXPERIMENTAL FACTORS AND CONSTRAINTS

A large number of factors could be considered in the optimization of the compression-molding process. However, the most relevant factors for the control of the

actual production are the charge area as a percentage of the mold area (A), the length-to-width ratio of the charge (L), and the position of the center of the charge as measured in centimeters from the bottom of the mold (P).

To set up and execute the computer experiments, several assumptions had to be made and a set of constraints imposed to limit the size and complexity of the optimization procedure. Throughout the experimentation, it was assumed that:

- All runs were made with a vertical mold closing speed of 1 centimeter/second.
- The mold was assumed to be flat and of uniform thickness.
- The charge volume was equal to the closed mold volume.
- The charge was of uniform thickness.
- Only one charge was allowed in the mold.
- The temperature of the mold was assumed to be constant.
- The charge was always rectangular in shape.

These assumptions were considered realistic and without major effect on the practical applicability of the experimental results.

OVERVIEW OF THE EXPERIMENTAL METHOD

Response surface methodology is a sequential approach to optimization that proceeds through several phases. For a systematic overview of RSM see [3]. Here we only provide a conceptual overview. The first phase of the optimization process consists of a series of small experiments, usually two-level factorials like that shown in Figure 5a. When analyzing a two-level factorial experiment, the main effect of a factor is usually defined as the average change in the response as the factor is changed from its low to its high level. Assessing the relative size of these main effects is typically the first step in the analysis. If the optimum factor settings are far from the initial conditions, the response surface is likely to be steep with relatively less curvature. In such cases, the main effects of the factors, which are two times the slope of the response function, are usually relatively large and provide adequate information to determine

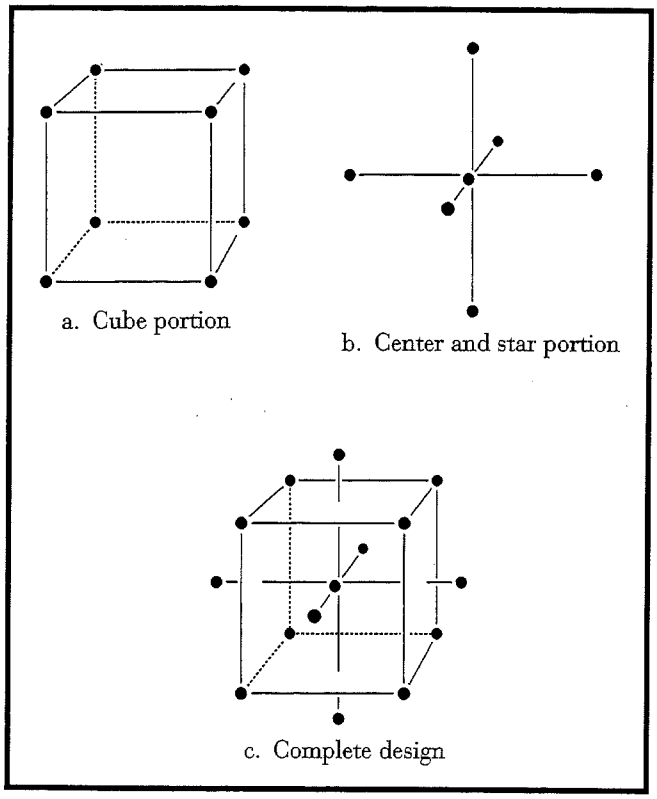

Fig. 5. A central composite design. (a) Cube portion; (b) center and star portion; (c) complete design.

the approximate direction of steepest ascent or descent. If large numbers of factors are being studied, fractional factorial designs can be used to reduce the number of experimental trials required for calculating the main effects [8].

The factor settings for each experiment are determined based on the direction of maximum benefit established in the preceding experiment. When the experiment is run, a new direction is established, and the cycle continues until a point of diminishing marginal return is reached. Most practical problems have multiple responses. Thus, we must judge the relative importance of each response to determine the direction of maximum benefit.

When near-optimal conditions are reached, there is usually relatively more curvature in the response surface. The second order derivatives are therefore likely to be relatively larger when compared to the first order terms. When this occurs, it marks the beginning of the second phase of a RSM study, in which a second order

polynomial model for the response needs to be estimated. Such models allow for more detailed study of curvature and possible determination of local optima, ridges, valleys, or other types of local properties. In order to estimate a second order model, two-level factorials are augmented with center and star points as indicated in Fig. 5b. The combined design shown in Fig. 5c, called a central composite design, is well suited for the estimation of second order models.

A key advantage of RSM over large, comprehensive, one-shot experiments, is the sequential nature of the decision-making. This approach allows the experimenter to gain as much knowledge as possible from a few initial trials before committing additional experimental resources. After each small experiment, the experimenter can reevaluate the factors, responses, and even objectives, thus allowing opportunities for creative thinking, balancing conflicting objectives, and reducing the number of wasteful trials.

In the compression-molding example to be discussed below, four experiments were designed and analyzed. The first three experiments were two-level, three-factor (2^3) factorial designs in which the levels of each factor in each experiment were set based on the insight gained from the analysis of the previous experiment. The fourth and last experiment was a central composite design built using the 2^3 (cube) design from the third experiment augmented by center and star points. As we started this particular project, the hood scoop was already in production, with charge location and size somewhat "optimized" based on experience. Thus, we used the current charge location and size as a starting point for our numerical optimization. In other cases, we may have to use our best judgment to determine a starting location.

THE EXPERIMENTAL PROGRESSION

We will now discuss the actual steps of our computer experiment for the finite element model of the hood scoop. A critical part of the response surface methodology approach is the human interaction with the model during the sequence of experiments. To emphasize this aspect, we will provide a detailed description of the experimental progression and the judgments and decisions that were reached at various stages.

Recall that we were using three factors, the charge area as a percentage of the mold area (A), the length-to-width ratio of the charge (L), and the position of the center of the charge as measured in centimeters from the bottom of the mold (P). Our starting point was the original charge, which had an area 16% the size of the mold area, a length-to-width ratio of 0.827, and a position of 20.6 centimeters from the bottom of the mold. For this starting point, the model predicted a fill time tolerance of 1.129 seconds and an average fiber orientation response of 0.849. Note that this last index was only a relative measure of "goodness," which in itself does not mean much, but can be compared with results from previous experiments to check for progress.

As already indicated, the first experiment was a 2^3 factorial set up near the original process conditions. At that stage, it was conjectured that larger charge areas, larger length-to-width ratios, and higher charge positions would produce better results. Therefore, the factor levels for the experiment were chosen in these directions with respect to the original charge. Figure 6 shows the relationship of the experimental design points of the first experiment to the original charge in the three-dimensional space spanned by x_A, x_L, and x_P, which are

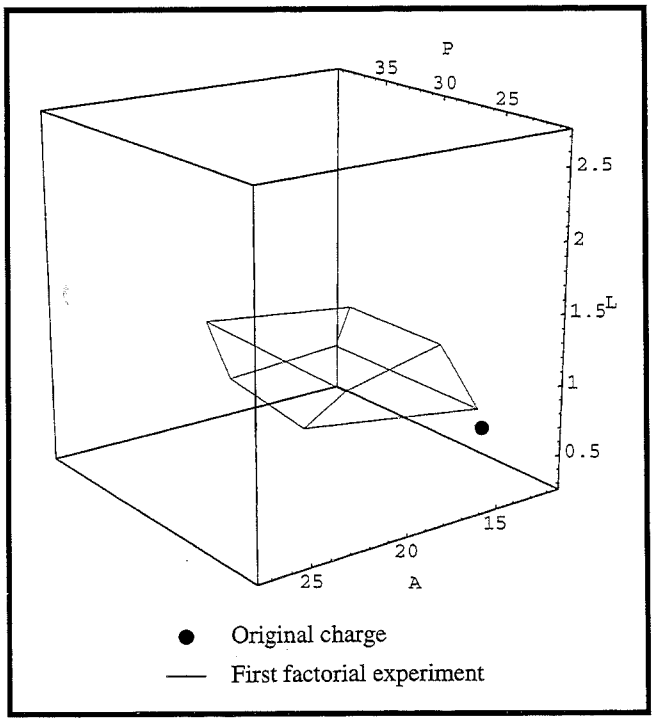

Fig. 6. The first experiment.

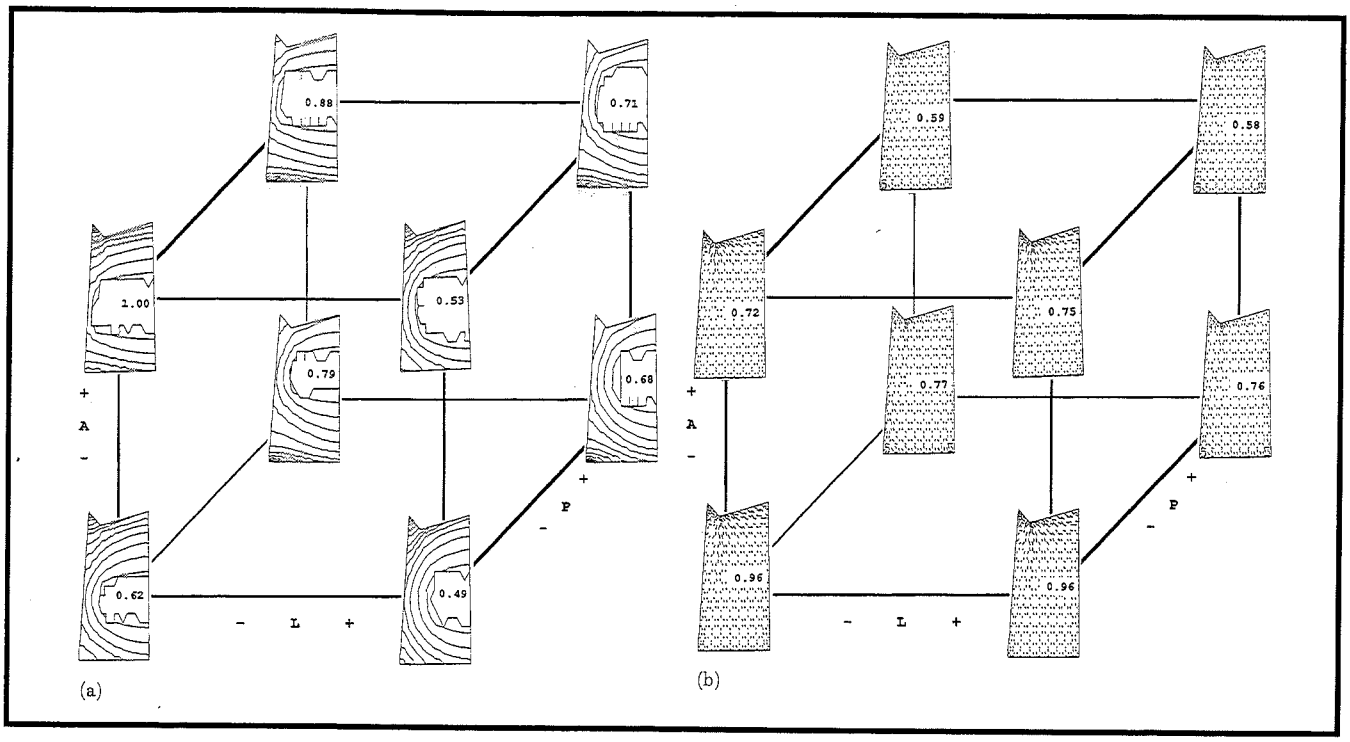

Fig. 7. (a) Cube plot of mold flow and fill time tolerance (Experiment 1); (b) cube plot of fiber orientation plots and average fiber orientation (Experiment 1).

the axes for the factors A, L, and P, respectively. Note that although the original 2^3 design would usually form a regular rectangular cuboid, the actual design geometry is somewhat distorted. The distortion is caused by the discrete nature of the finite element mesh. Thus A, L, and P cannot be changed completely at will. In most cases, small deviations from the standard design will have little effect on the data analysis. However, if these deviations become large many of the standard graphical and statistical methods used to analyze two-level factorials become less useful and multiple linear regression techniques should instead be used.

Graphical methods, like those presented in [9], were used for the analysis of the first experiment. In particular, cube plots with both the pictorial and quantified responses on each corner (see Figure 7) helped to determine the direction of steepest descent for each response and a suitable compromise direction for proceeding to the next experiment. Also, dot plots were made of the main effects and interaction effects, which measure the amount that the main effect of a certain factor changes when a second factor is varied [9]. For example, AP represents the interaction effect which measures the change in the main effect of A when the P is changed from low to high. The dot plots, shown in Figure 8, were used to compare the relative sizes of the effects. Ideally, such dot plots show a cluster of small, relatively unimportant effects located near zero and a few larger, more important effects distributed further away from zero. Thus, the dot plots help to identify which factors have a large effect on the quantified responses.

From the dot plot in Fig. 8a, we decided that L was the factor which was most important for reducing the fill time tolerance. Since L had little or no effect on the other responses, L was increased for the second set of experiments. In fact it was increased substantially because it was conjectured that the charge ought to resemble the shape of the mold which has a much higher length-to-width ratio than the original charge.

Figure 8b is the corresponding dot plot of effects on average fiber orientation. It shows that increasing factor A had a large negative effect. Therefore, since the objective was to decrease the fiber orientation to obtain

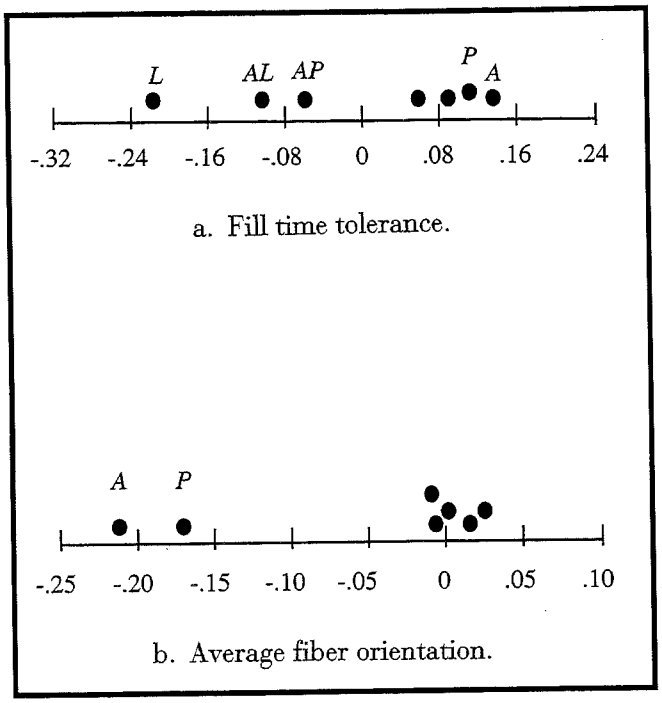

Fig. 8. Dot plots of effects (Experiment 1). (a) Fill time tolerance; (b) Average fiber orientation.

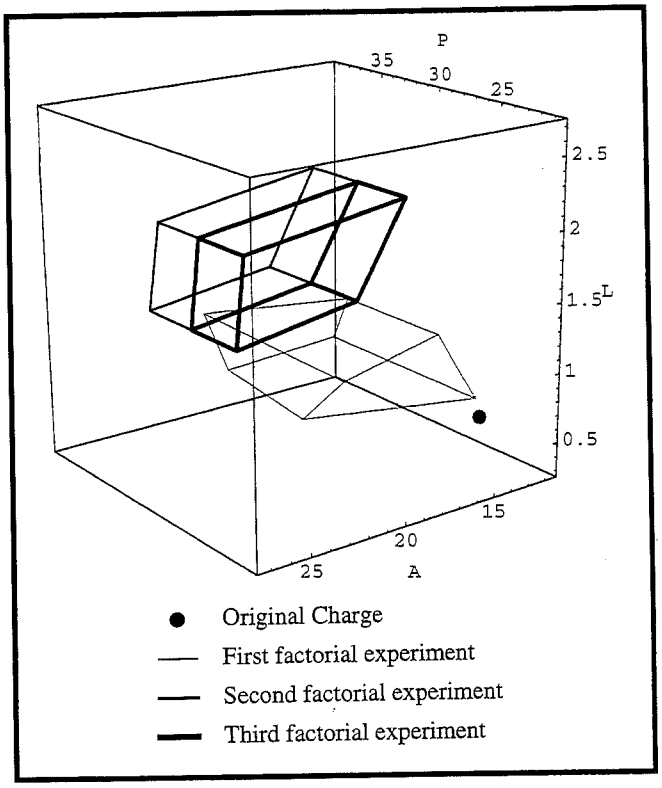

Fig. 9. The factorial experiments.

a more random pattern, we decided to increase this factor in the second experiment. However, the increase was limited because the charge area was constrained to be less than 30% of the mold area.

The cube plot in Fig. 7a shows that when the charge was placed in the upper part of the mold, the flow front always reached the upper edge of the mold long before it reached the lower edge of the mold. When the charge was low in the mold, the converse happened. This imbalance in the filling of the upper and lower edges of the mold caused the fill time tolerance to be large. Thus, it was decided that the range used for varying P was too large.

The second experiment, also a 2^3 design, was set up based on the findings stated above. Its relative position to the first experiment in the x_A, x_L, and x_P space is indicated in Figure 9. During the second experiment, the average fiber orientation response was found to be unstable as it was currently being calculated. In order to reduce computation time in the first experiment, the convective derivative from the fiber orientation model had been dropped and only the last steps of the mold-filling were included in the fiber orientation calculation. This required the experimenter to select the number of nodes that were considered to be the last to fill based on the filling pattern computed by the simulation program. However, during the second experiment, we noticed that the average fiber orientation was quite sensitive to the number of nodes chosen by the experimenter. Varying the number of nodes used was enough to change a trial from among the best to among the worst runs in the entire experiment with respect to average fiber orientation. Therefore, since the average fiber orientation was so sensitive to a relatively arbitrary decision, we lost confidence in this measure as a reliable optimization criterion. We felt that the value of this second numerical response was not worth the additional calculation time for adding back the convective derivative. We therefore discontinued the use of the average fiber orientation as a response.

Having eliminated the average fiber orientation, the minimization of the fill time tolerance now became our key objective. The analysis of the cube plot showed that in every trial of the second experiment, the flow front reached the top of the mold long before it reached

the bottom, thus increasing the fill time tolerance. This indicated that the levels selected for the position, P, were too high and should be reduced.

The third experiment was set up based on the analysis from the second experiment. The same levels of A and L as in the second experiment were used. However, lower levels of P were chosen because the second experiment showed that positions near the center of the mold (x_P = 33 centimeters) reduced the fill time tolerance. Thus, the two levels of position for the third experiment were set at 29 and 34 centimeters, respectively. This "centering" can be seen in Fig. 9, which shows the spatial location of the third experiment relative to the first and the second experiments.

The results of the third factorial experiment showed that we had now significantly improved the fill time tolerance. Using the original charge, the predicted fill time tolerance had been 1.129 seconds; the range of predicted fill time tolerances from the first experiment was 0.49 to 1.00 seconds, and the range from the second experiment was 0.36 to 1.52. For the third experiment, this range had dropped, and was 0.35 to 0.64 seconds. Also, the dot plot of effects for experiment three was made and is shown in Figure 10. We see that several of the interaction effects are of the same magnitude or larger than the main effects. Both the drop in the range of the response and the increased relative magnitude of the interaction effects indicate that an optimum might be close and that it would be appropriate to move on to the second phase of experimentation using second order models.

The objective of the fourth experiment was to model the response "fill time tolerance" using a second order model. The factorial design from the third experiment was augmented with a center point and six star points to form a central composite design. Figure 11 shows the fourth experiment and the spatial location of

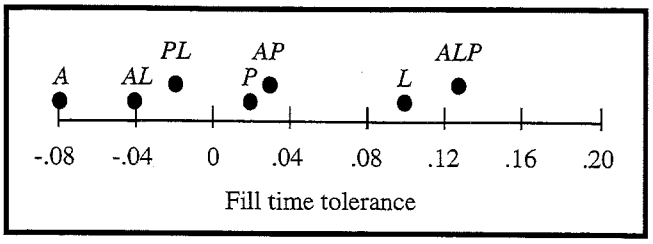

Fig. 10. Dot plot of effects (Experiment 3). Fill time tolerance.

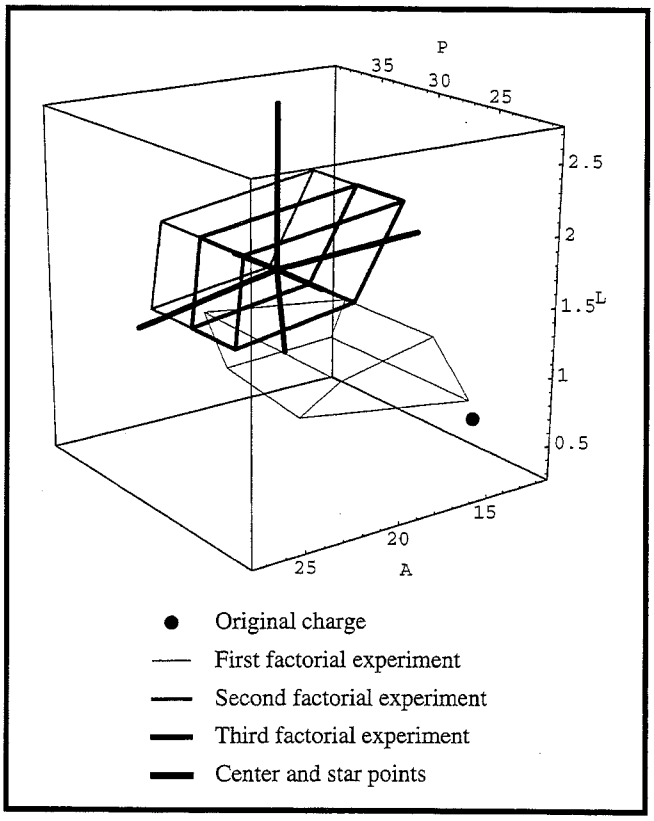

Fig. 11. The entire experimental progression.

the entire experimental progression. As in the previous experiments, it was not possible to choose the factors entirely at will due to the discrete nature of the finite element mesh. The design, therefore, is not exactly a central composite design. In the first three experiments, this slight distortion of the design was found to have little effect on the analysis. However, with the more complicated central composite design, the design distortion was more important and the analysis was carried out using multiple linear regression techniques.

THE NEAR OPTIMUM RESPONSE SURFACE

As mentioned above, fill time tolerance is defined as a measure proportional to the standard deviation of the filling times of the boundary nodes. To stabilize the variance of this response [7], it was therefore suggested that the fill time tolerance be transformed by taking its natural logarithm before fitting the second order model. This transformation would have been appropriate earlier in the experimentation, but was not suggested until this point in the experimental progression. After this

Table 1. The Design Points and Data from the Fourth Experiment

Trial #	x_A	x_L	x_P	Fill Time Tol (FTT) (seconds)	ln(FTT)
1	15.6	1.29	30.8	0.357	−1.030
2	23.2	1.25	28.8	0.409	−0.895
3	14.1	2.06	28.8	0.643	−0.442
4	21.9	1.80	30.8	0.370	−0.994
5	15.6	1.29	35.0	0.491	−0.711
6	23.2	1.25	33.0	0.361	−1.018
7	14.1	2.06	33.0	0.495	−0.703
8	21.9	1.80	35.0	0.523	−0.648
9	18.8	1.55	33.0	0.362	−1.017
10	11.7	1.71	31.0	0.465	−0.766
11	27.3	1.44	31.0	0.311	−1.167
12	19.5	1.03	31.0	0.422	−0.863
13	18.7	2.74	33.0	0.596	−0.518
14	18.8	1.54	28.9	0.481	−0.733
15	18.8	1.54	37.1	0.693	−0.367

transformation, the data (Table 1) were fit to a second order model of the form:

$$w = b_0 + \sum_{i=1}^{3} b_i x_i + \sum_{i=1}^{3}\sum_{j=1}^{3} b_{ij} x_i x_j + \varepsilon$$

$$= b_0 + b_1 x_A + b_2 x_L + b_3 x_P + b_{12} x_A x_L + b_{13} x_A x_P$$

$$+ b_{23} x_L x_P + b_{11} x_A^2 + b_{22} x_L^2 + b_{33} x_P^2 + \varepsilon \quad (1)$$

where w is the natural log of the fill time tolerance and is an error term. The model, fitted by standard regression methods, is:

$$w = 25.58 - 0.101 x_A - 0.138 x_L - 1.60 x_p - 0.027 x_A x_L$$

$$+ 0.005 x_A x_p + 0.001 x_L x_P - 0.0005 x_A^2$$

$$+ 0.227 x_L^2 + 0.024 x_P^2 + \varepsilon \quad (2)$$

In order to interpret this surface, a canonical analysis was performed. (For details see Appendix 1). The analysis showed that the surface has a minimum along two canonical axes and a slight maximum along the third. Hence, it is a generalized saddle-shaped surface. In practical terms, for any given value of area, A_0, there is a setting for L and P which will minimize the fill time tolerance. Using Eqs. (A10) and (A11) in Appendix 1, Table 2 shows these optimum settings for several values of A_0. In the first column, A_0, the percent area of the charge can represent the half-charge with respect to the half-mold or the actual charge with respect to the full mold. The second column shows L_{opt}, the optimum length-to-width ratio given A_0. Since the length-to-width ratio used is half of the length-to-width ratio of the actual charge in the full mold, the third column of Table 2 was added showing the optimum length-to-width ratio of the charge in the full mold. The fourth column shows P_{opt}, the optimum position given A_0. The last column gives the expected value of the fill time tolerance at the levels specified for A_0, L_{opt}, and P_{opt}. Note that these equations are only valid within a small region around the optimal conditions.

In order to get a geometric understanding of the response surface near its optimum, a three-dimensional plot of a surface contour of the response was created. Figure 12 shows the surface contour where fill time tolerance is equal to 0.4 seconds. The region inside this surface is where fill time tolerance is minimized. Thus, for any given value of $x_A = A_0$, the minimum response will be at the center of the surface contour.

By studying the results summarized in Table 2 and the surface of Fig. 12, the following conclusions

Table 2. The Predicted Optimum and Optimal Settings for L and P given a Charge Area A_0

A_0	L_{opt} (1/2 MOLD)	L_{opt} (FULL MOLD)	P_{opt} (CM)	EXPECTED Fill Time Tol. (seconds)
10	0.81	0.41	32.7	0.37
12	0.93	0.46	32.5	0.38
14	1.05	0.52	32.3	0.38
16	1.16	0.58	32.1	0.38
18	1.28	0.64	31.9	0.38
20	1.40	0.70	31.8	0.37
22	1.51	0.76	31.6	0.35
24	1.63	0.81	31.4	0.34
26	1.75	0.87	31.2	0.32
28	1.86	0.93	31.0	0.30

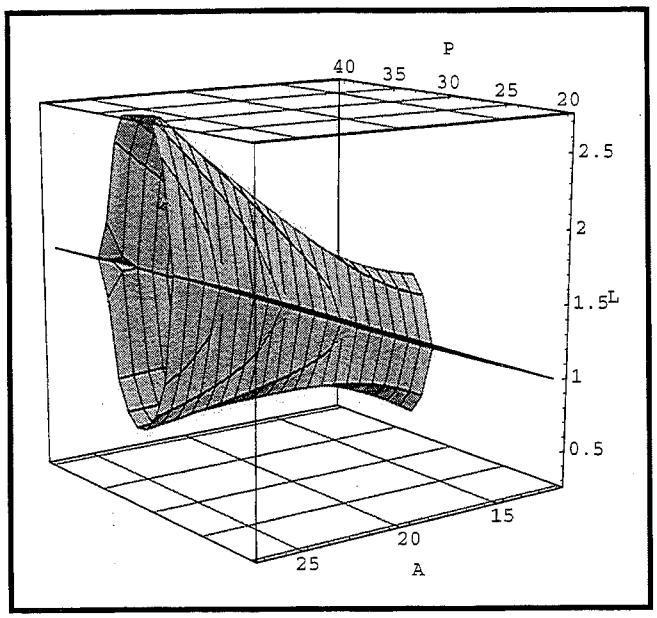

Fig. 12. The response surface contour (fill time tolerance = 0.4 seconds).

were reached concerning the behavior of fill time tolerance in the region of the third and fourth experiments:

- The response surface in Fig. 12 reveals that the area of minimum fill time tolerance increases as the charge area increases. This means that for large charge areas the importance of the shape and location of the charge is reduced. Thus, if it is costly to control the shape or location of the charge in production, a large charge area could be used and the other factors could be allowed to vary without significantly affecting the uniformity of the mold-filling.
- The last column of Table 2 shows that the relative difference in time between the minimum fill time tolerance of the large charge and that of the small charge is most likely insignificant. Therefore, small charge areas can be used without seriously reducing the uniformity of the mold filling. However, it will require tighter control of the factors L and P to obtain the minimum fill time tolerance with small charge areas.
- Noting that the center of the mold is located at a position of 33 centimeters, column four of Table 2 shows that the optimum position is close to the center and does not change much with charge area. Thus, the charge should be centered regardless of size. This is a reasonable and, in retrospect, an expected result.
- The third column of Table 2 indicates that a 1:2 length-to-width ratio is optimal when a small charge area is used. However, as the charge area increases, the optimum charge shape begins to approach a square to match the mold's shape. This result was not obvious and may provide valuable insight into the system dynamics of the actual physical process used for prototype testing.

Note that the simulation does not give any prediction of surface characteristics. Thus, the most useful way to use the results of the above model optimization is to choose a charge area which gives the best possible surface characteristics. Then given the charge area, we recommend using the corresponding length-to-width ratio given in Table 2 and placing the charge in the center of the mold. Thus, a starting point for physical prototype testing has been located and the analysis has provided some general understanding of the system to aid in that testing.

CONCLUSION

Creating a computer model is an important first step for designing quality into a product or process. However the next logical step is to optimize that model. Here engineers may, for lack of a better method, resort to a "try this-try that" one-factor-at-a-time approach. In this article, we have discussed an alternative method for computer experimentation and model optimization based on iterative learning which we, through several practical applications, have found valuable. Used sequentially, RSM can save time and more often leads to optimal solutions and better understanding.

It may be suggested that our approach be developed into a fully automated algorithm, which would eliminate the human interaction at each step of the experiment. However, we are hesitant to promote such an approach. The human interaction and application of common sense judgment at each step is important because sometimes new aspects of the model's behavior is learned which may change our objectives or give us new ideas. It was for this reason that we included details of

the experimental progression including the elimination of a response and our realization, only at the last step of experimentation, that the log transformation would be appropriate for our remaining response. We have found that the experimenter can balance the objectives and constructively interface with the computer model and, thus, reduce the risk of inappropriate solutions.

ACKNOWLEDGMENTS

The authors would like to thank Jose Castro and his associates at GenCorp, Inc. for their help in explaining the compression molding process and their interest in the project. We would also like to thank Dr. Toby Mitchell who provided valuable insights on the experimental design issues. The work on this article was supported by National Science Foundation Grants DDM-8808138 and ECD-87211545 and a grant from the Alfred P. Sloan Foundation.

REFERENCES

1. Sacks J., Welch W. J., Mitchell T. J., and Wynn H. P., Design and Analysis of Computer Experiments, *Statistical Science* **4**: 409–422, 1989.
2. Box G. E. P. and Wilson K. B., On the Experimental Attainment of Optimum Conditions, *J. Roy. Stat. Soc. B*, **13**: 1–45, 1951.
3. Box G. E. P. and Draper N. R., *Empirical Model Building and Response Surfaces*, John Wiley & Sons, New York, 1987.
4. Myers R. H., Khuri A. I., and Carter W. H., Jr., Response Surface Methodology: 1966–1988, *Technometrics*, **31:** 137–157, 1989.
5. Osswald T. A. and Tucker C. L., III, Compression Mold Filling Simulation for Non-Planar Parts using the Finite Element/Control Volume Approach, *International Polymer Processing*, **5:** 79–87, 1990.
6. Folgar F. and Tucker C. L., III, Orientation Behavior of Fibers in Concentrated Suspensions, *J. Reinf. Plast. and Comp.*, **3:** 98–119, 1984.
7. Natrella M. G., *Experimental Statistics*, National Bureau of Standards, Washington, D. C. pages 20–6 to 20–8, 1963.
8. Box G. E. P., Hunter W. G., and Hunter J. S., *Statistics For Experimenters*, John Wiley & Sons, New York, 1978.
9. Box G. E. P., Hunter W. G., and Hunter J. S., *Statistics For Experimenters*, John Wiley & Sons, New York, 1978.
10. Myers R. H., *Response Surface Methodology*, Allyn and Bacon, Inc., Boston, MA, 1971.

APPENDIX 1

The data of Table 1 were fit to a second order model of the form:

$$w = b_0 + \mathbf{b}'\mathbf{x} + \mathbf{x}'\mathbf{B}\mathbf{x} + \varepsilon \qquad \text{(A1)}$$

where w is the natural log of the fill time tolerance, ε is an error term, $\mathbf{x}' = (x_A, x_L, x_P)$, $\mathbf{b}' = (b_1, b_2, b_3)$, and

$$\mathbf{B} = \begin{bmatrix} b_{11} & \frac{1}{2}b_{12} & \frac{1}{2}b_{13} \\ \frac{1}{2}b_{12} & b_{22} & \frac{1}{2}b_{23} \\ \frac{1}{2}b_{13} & \frac{1}{2}b_{23} & b_{33} \end{bmatrix}.$$

A second order response surface model like the one shown in (A1) can be difficult to interpret. The geometric shape of the surface is not readily apparent from the coefficients in the model. By reexpressing the model in canonical form, which corresponds to relocating the coordinate system at the stationary point of the fitted response surface and appropriately rotating the axes, the interpretation is greatly simplified [3, 10]. In the canonical form, the response surface model is expressed in pure quadratic terms in an equation of the form:

$$w = \hat{w}_s + \mathbf{z}'\Lambda\mathbf{z} + \varepsilon \qquad \text{(A2)}$$

where $\mathbf{z}$ is a new three dimensional axis system, $\mathbf{z}' = (z_1, z_2, z_3)$, $\hat{w}_s$ is predicted response at the stationary point, and Λ is a 3x3 diagonal matrix. The origin of the $\mathbf{z}$ axis system is the stationary point of (A1) and is given by:

$$\mathbf{x}_s = -\tfrac{1}{2}\mathbf{B}^{-1}\mathbf{b} \qquad \text{(A3)}$$

The three eigenvalues of $\mathbf{B}$ are the diagonal terms of Λ and the corresponding eigenvectors of $\mathbf{B}$, $\mathbf{m}_1$, $\mathbf{m}_2$, and $\mathbf{m}_3$, are formed into a matrix, $\mathbf{M}$, as follows: $\mathbf{M} = [\mathbf{m}_1, \mathbf{m}_2, \mathbf{m}_3]$. The $\mathbf{x}$ axes system is then rotated and shifted to form the $\mathbf{z}$ axes by the following equation:

$$\mathbf{z} = \mathbf{M}'(\mathbf{x} - \mathbf{x}_s) \qquad \text{(A4)}$$

In the form of (A2), the fitted surface for w is:

$$\hat{w} = -0.97 + 0.228z_1^2 + 0.024z_2^2 - 0.001z_3^2 \qquad \text{(A5)}$$

With the response equation in this form, a few observations can give a geometric understanding of the response surface and its minimum. First, note the signs of the coefficients. Since the coefficients for z_1 and z_2 are positive, $\hat{w}$ will be minimum when z_1 and z_2 are zero,

that is, on the z_3-axis. The equation for the predicted response on the z_3-axis is then:

$$\hat{w} = -0.97 - 0.001z_3^2 \qquad \text{(A6)}$$

Since the sign of the coefficient for z_3 is negative, the response on the z_3-axis is maximum at $z_3 = 0$, the stationary point. We also note that the coefficient of z_3 is relatively small. It may be that the amount that the response changes along the z_3-axis is not practically significant.

The inverse of the **M′** matrix is **M**. Thus, Eq. (A4) can be rearranged as follows:

$$\mathbf{x} = \mathbf{Mz} + \mathbf{x}_s \qquad \text{(A7)}$$

With z_1 and z_2 set to zero, (A7) becomes

$$\mathbf{x} = \mathbf{m}_3 z_3 + \mathbf{x}_s, \qquad \text{(A8)}$$

where, for this example,

$$\mathbf{m}_3 = \begin{bmatrix} -0.994 \\ -0.058 \\ 0.090 \end{bmatrix} \text{ and } \mathbf{x}_s = \begin{bmatrix} 15.0 \\ 1.1 \\ 32.2 \end{bmatrix}.$$

Since z_3 is a linear combination of the physical factors, it is hard to choose a z_3 which has intuitive meaning. Instead, a charge area, A_0, is chosen. Using (A8), the value of z_3 on the z_3-axis which has a charge area of A_0 can be calculated to be:

$$z_3 = -1.006A_0 + 15.13 \qquad \text{(A9)}$$

Using (A8) and (A9), the values of L and P which would be on the z_3-axis at the point where $x_A = A_0$ and, thus, an optimum for the given A_0 can be found. These values, called L_{opt} and P_{opt}, can be calculated using the equations below:

$$L_{opt} = 0.058A_0 + 0.23 \qquad \text{(A10)}$$

$$P_{opt} = -0.090A_0 + 33.57 \qquad \text{(A11)}$$

These equations are used to create Table 2, which is helpful in the interpretation of the near-optimal conditions.

Søren Bisgaard is the director at the Center for Quality and Productivity Improvement and associate professor in the Department of Industrial Engineering, University of Wisconsin-Madison. He holds two engineering degrees in industrial and manufacturing engineering and MS and PhD degrees in statistics from the University of Wisconsin-Madison. Before entering the university, he worked for several years as a machinist/toolmaker for companies in Denmark and Germany. Dr. Bisgaard has worked as an industrial consultant in quality improvement, operations research, and managerial accounting. He is a co-author with George Box and Conrad Fung of the video series "Designing Industrial Experiments." Dr. Bisgaard's research ideas are in the areas of experimental design, the use of statistics for designing better quality into products and processes, quality control, quality management, and concurrent engineering. He has received both the Shewell and Brumbaugh Awards from the American Society for Quality Control. In 1990 Dr. Bisgaard received the Ellis R. Ott Award for excellence in quality improvement.

Bruce Ankenman is a research assistant at the Center for Quality and Productivity Improvement and a PhD student in the Quality Engineering Program in the Department of Industrial Engineering, University of Wisconsin-Madison. He holds a BS degree in electrical engineering from Case Western Reserve University and an MS degree Manufacturing Systems Engineering from University of Wisconsin. Before returning for graduate studies, he worked for five years as a product design engineer for an automotive supplier in Ohio.

Tim A. Osswald received his PhD in mechanical Engineering at the University of Illinois at Urbana-Champaigne in the field of Polymer Processing. He spent two and one-half years at the Institute of Plastics Processing (IKV) in Aachen, West Germany, as an Alexander von Humboldt Fellow. He joined the faculty